The Influence of Topography on Convective Storm Environments in the Eastern United States as Deduced from the HRRR

BRANDEN KATONA AND PAUL MARKOWSKI

Department of Meteorology, The Pennsylvania State University, University Park, Pennsylvania

CURTIS ALEXANDER AND STANLEY BENJAMIN

NOAA/Earth System Research Laboratory/Global Systems Division, Boulder, Colorado

(Manuscript received 29 February 2016, in final form 21 May 2016)

ABSTRACT

Relatively little is known about how topography affects convective storms. The first step toward understanding these effects is to investigate how topography affects storm *environments*. Unfortunately, the effects of topography on convective environments are not easily observed directly. Instead, it is necessary to resort to using output from the High-Resolution Rapid Refresh (HRRR). The HRRR's 3-km grid spacing can resolve some of the larger-scale topographic effects. Popular convective storm forecasting parameters obtained from the HRRR are averaged on convective days from February to September 2013–15. It is surmised that most of the day-to-day variability attributable to synoptic- and mesoscale meteorological influences is removed by averaging; the remaining horizontal heterogeneity in parameters related to instability and vertical wind shear is due to the hemispheric-scale meridional temperature and pressure gradient, and likely also topographic influences, especially where recurring longitudinal variations in instability, wind shear, etc. are found. Anomalies are sensitive to the ambient low-level wind direction (i.e., whether winds are locally blowing upslope or downslope), especially for parameters that depend on the low-level vertical shear. The statistical significance of local maxima and minima is demonstrated by comparing the amplitudes of the anomalies to bootstrapped estimates of the standard errors.

1. Introduction

Convective storms regularly occur in regions of complex topography, such as the eastern United States and Europe. A growing number of observational studies speculate that terrain has an important influence on the analyzed storms (Teng et al. 2000; LaPenta et al. 2005; Bosart et al. 2006; Tang et al. 2016). It is widely acknowledged that topography can influence storms, but that it is difficult to say how, in part, because it can never be known how an observed storm would have behaved in the absence of terrain. For this reason, a number of studies have used idealized simulations to study the influence of topography on storms (Homar et al. 2003; Frame and Markowski 2006; Ćurić et al. 2007; Reeves and Lin 2007; Markowski and Dotzek 2011; Soderholm et al. 2014). To date, simulations have featured both *idealized storms* and *idealized terrain*, making it difficult for forecasters to know how particular terrain features in their areas of responsibility might affect storms. There is an obvious need to 1) understand how topography affects storm environments and 2) understand how these environmental modifications affect storms. This paper deals with the first of these needs.

Our approach is to average instability and wind shear parameters commonly used in forecasting convection obtained from the High-Resolution Rapid Refresh model (HRRR; Smith et al. 2008; Benjamin et al. 2016). The synoptic and mesoscale variability not due to topography ought to become greatly diminished in the

Supplemental information related to this paper is available at the Journals Online website: http://dx.doi.org/10.1175/WAF-D-16-0038.s1.

Corresponding author address: Branden Katona, Dept. of Meteorology, The Pennsylvania State University, 503 Walker Bldg., University Park, PA 16802.
E-mail: katona@psu.edu

DOI: 10.1175/WAF-D-16-0038.1

mean fields, such that the remaining variability would represent mostly standing patterns of topographically generated variability, along with a smaller contribution from the hemispheric-scale mean meridional temperature and pressure gradients, as well as any systematic errors potentially present in the HRRR (such as the assimilation of biased surface observations). Explaining the dynamical origins of the virtually countless anomalies present in the mean fields is beyond the scope of this paper. Rather, the goal of this paper is to expose avenues for future research geared toward understanding the possible influence of topography on convective storm behavior. In section 2, we discuss the methodology in greater detail. Section 3 presents some mean HRRR fields of popular severe weather forecasting parameters and identifies some geographic locations where a significant topographic influence is likely. Conclusions and some thoughts on future work are presented in section 4.

2. Data and methods

Climatologies of popular convective storm forecasting parameters on convective storm days (to be defined below) in the northeast and southeast United States (Figs. 1a,b) were constructed from the HRRR model of NOAA's Earth System Research Laboratory. The HRRR has a 3-km horizontal grid spacing, which is expected to be adequate for resolving the largest mesoscale influences of topography on convective storm environments. (By comparison, the spatial and temporal resolution of the U.S. rawinsonde network is grossly inadequate for detecting terrain influences on convective storm environments.)

A sufficiently large sample of environments is necessary to ensure that day-to-day synoptic and mesoscale variability not due to topographic influences mostly vanishes. For example, fields of CAPE, shear, etc. typically have synoptic and mesoscale variations independent of terrain (e.g., low-level shear is commonly maximized in a meridional axis coincident with a low-level jet stream ahead of an approaching cold front). In mean fields of environmental parameters derived from a large sample of cases, the variability is expected to represent topographically induced variability and the influence of the hemispheric-scale meridional temperature/pressure gradient.

HRRR forecasts were obtained from the 1 February to 30 September 2013–15 period. The HRRR model configuration remained relatively stable, including both the data assimilation system and model physics, from 2013 to 2015 (the experimental ESRL HRRR was used for 2013–14 and the operational NCEP HRRR was used for 2015 in order to maintain stability in the model configuration). One risk in using a longer window of HRRR fields would be the potential for the climatologies to be adversely affected by significant changes to the model that are inevitable over a much longer period of time. The changes to the HRRR configuration from 2012 to 2013 and from 2015 to 2016 are substantial enough that extending the analysis beyond the 2013–15 period may introduce unwanted sources of variability in the climatologies.

Climatologies of the mixed layer convective available potential energy (MLCAPE), 0–1-km storm-relative helicity (SRH01; Davies-Jones et al. 1990), and fixed-layer significant tornado parameter (STP; Thompson et al. 2003) are presented in this paper. CAPE is a measure of the vertically integrated buoyancy that can be realized by an updraft and is, therefore, related to the updraft speeds. MLCAPE is calculated using the average equivalent potential temperature of the three lowest 30-hPa layers. SRH01 is the vertically integrated product of streamwise vorticity and storm-relative wind speed in the lowest kilometer [storm motions are obtained from the Bunkers et al. (2000) algorithm], and has been shown to be a good predictor of both updraft rotation and tornado formation [assuming adequate CAPE is present; e.g., Thompson et al. (2003)]. STP, which combines CAPE, SRH01, cloud-base height, and 0–6-km shear, has been shown to be an even better discriminator than SRH01 between nontornadic supercells and supercells that produce significant [(enhanced Fujita scale) EF2+] tornadoes. STP is calculated similar to the Thompson et al. (2003) formulation, but MLCAPE and mixed-layer lifted condensation level heights (MLLCLs) are replaced by surface-based CAPE and LCL heights.

The climatologies were created using 2-h HRRR forecasts of the parameters rather than 0-h forecasts (analyses). Averaging 2-h forecasts from the HRRR instead of 0-h analyses ensures physical consistency within the three-dimensional model dynamics and parameterizations, and minimizes the effects of systematically biased surface station observations while minimizing forecast error. Climatologies were also created from 0-h analyses, but the mean fields contained features that looked unphysical, such as ''pockets'' of high MLCAPE surrounding some surface stations known to have systematic dewpoint biases.

Because the effects of terrain on airflow (and ultimately severe weather forecasting parameters) depend on the stratification, it seems sensible only to include stratifications that are associated with environments capable of supporting convection rooted in the boundary layer. A given day is included in the climatologies if

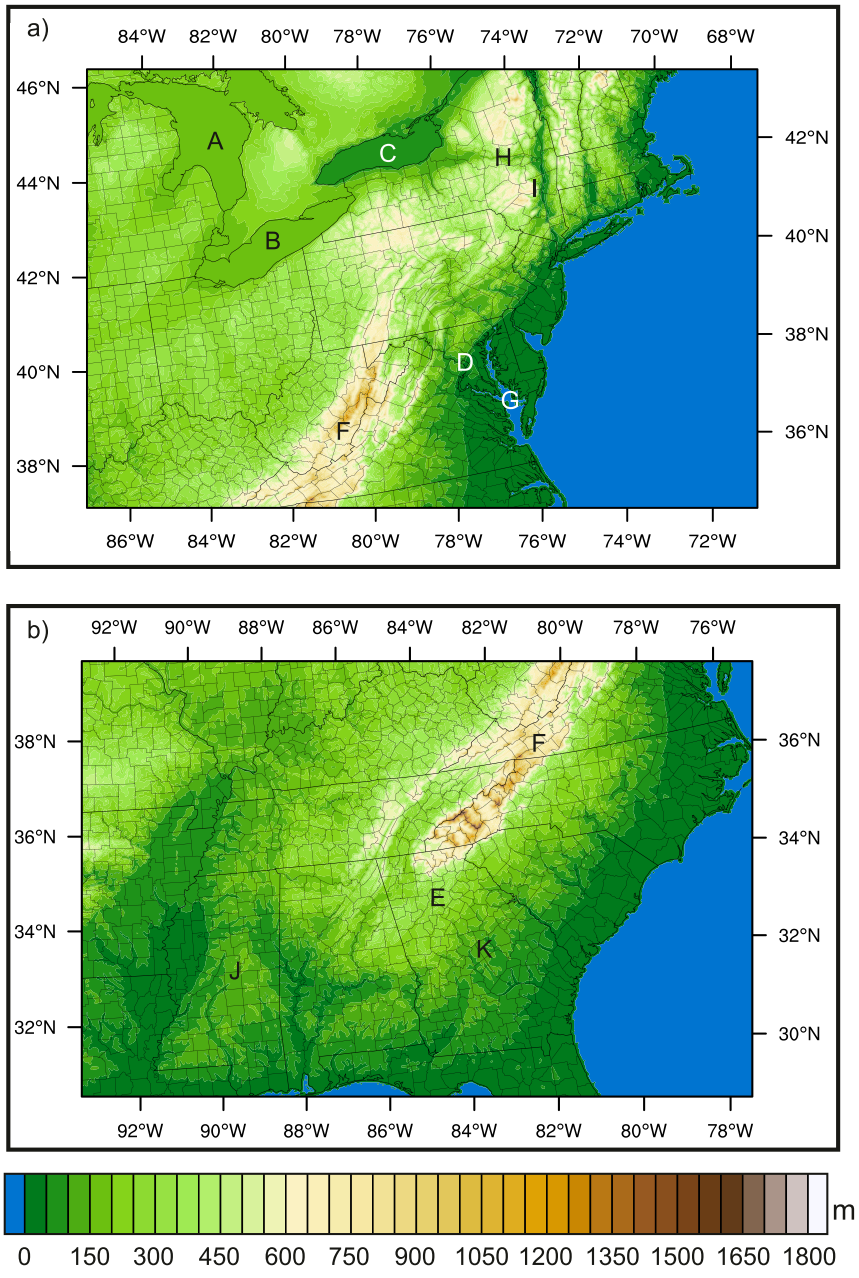

FIG. 1. Geopotential height (m) of the HRRR lower boundary in (a) the Northeast region and (b) the Southeast region. Capital letters represent Lake Huron (A), Lake Erie (B), Lake Ontario (C), Washington, D.C. (D), Atlanta, GA (E), the Appalachian Mountains (F), the Chesapeake Bay (G), the Mohawk Valley (H), the Hudson Valley (I), Mississippi (J), and Georgia (K).

MLCAPE exceeds 500 J kg^{-1} in 10% of the region's grid points over land (Fig. 1). All grid points within the region are included in the averages on such "convective storm days." The Northeast region (Fig. 1a) climatology encompasses 282 convective days while the Southeast region (Fig. 1b) climatology includes 395 days. Sensitivity tests demonstrated that varying the MLCAPE threshold value and percentage of the region exceeding it did not significantly alter the observed patterns, nor did only including grid points where MLCAPE exceeds 0 J kg^{-1}.

Though most aspects of convective storm dynamics are independent of the ground-relative winds and only depend on the storm-relative winds (Markowski and

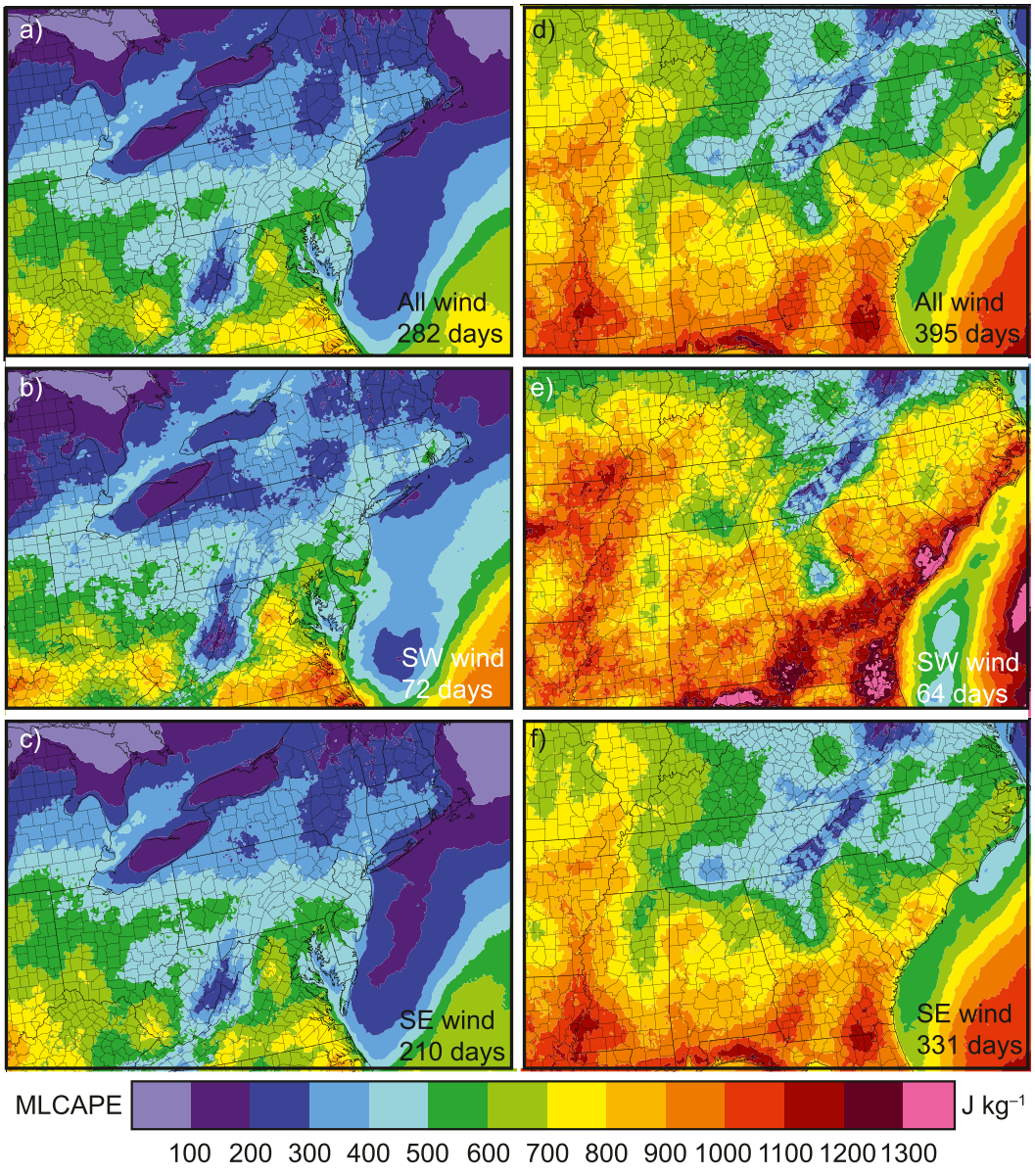

FIG. 2. Mean MLCAPE on convective days between 1 Feb and 30 Sep 2013–15 for (a),(d) all days, (b),(e) SW-flow days, and (c),(f) SE-flow days in the (left) Northeast and (right) Southeast regions.

Richardson 2006), the ground-relative wind profile is of leading-order importance in determining the impact of the underlying topography on the storms that cross it. The ground-relative wind profile dictates where the winds will blow upslope or downslope, which controls to a large extent the manner in which the environment is modified (Markowski and Dotzek 2011). Thus, the magnitude and perhaps even the sign of the topography-induced perturbations in the convective environment likely depend on the low-level wind direction. For this reason, the convective days were partitioned into southwesterly (SW) and southeasterly (SE) low-level flow bins, with the low-level flow direction defined by the mean 10-m wind in regions of positive MLCAPE. The use of 10-m winds instead of 925- or 850-mb winds does not change the results qualitatively. Because the Appalachian Mountains (these and other geographical locations referenced in the text are labeled in Fig. 1) are roughly oriented from 210° to 30°, 210° rather than 180° is used to separate the SW and SE flow regimes (it was felt that each bin should contain days in which the low-level flow impinges upon the terrain from the same side assuming a common orientation to the terrain ridge axes). Our binning strategy should not imply that only

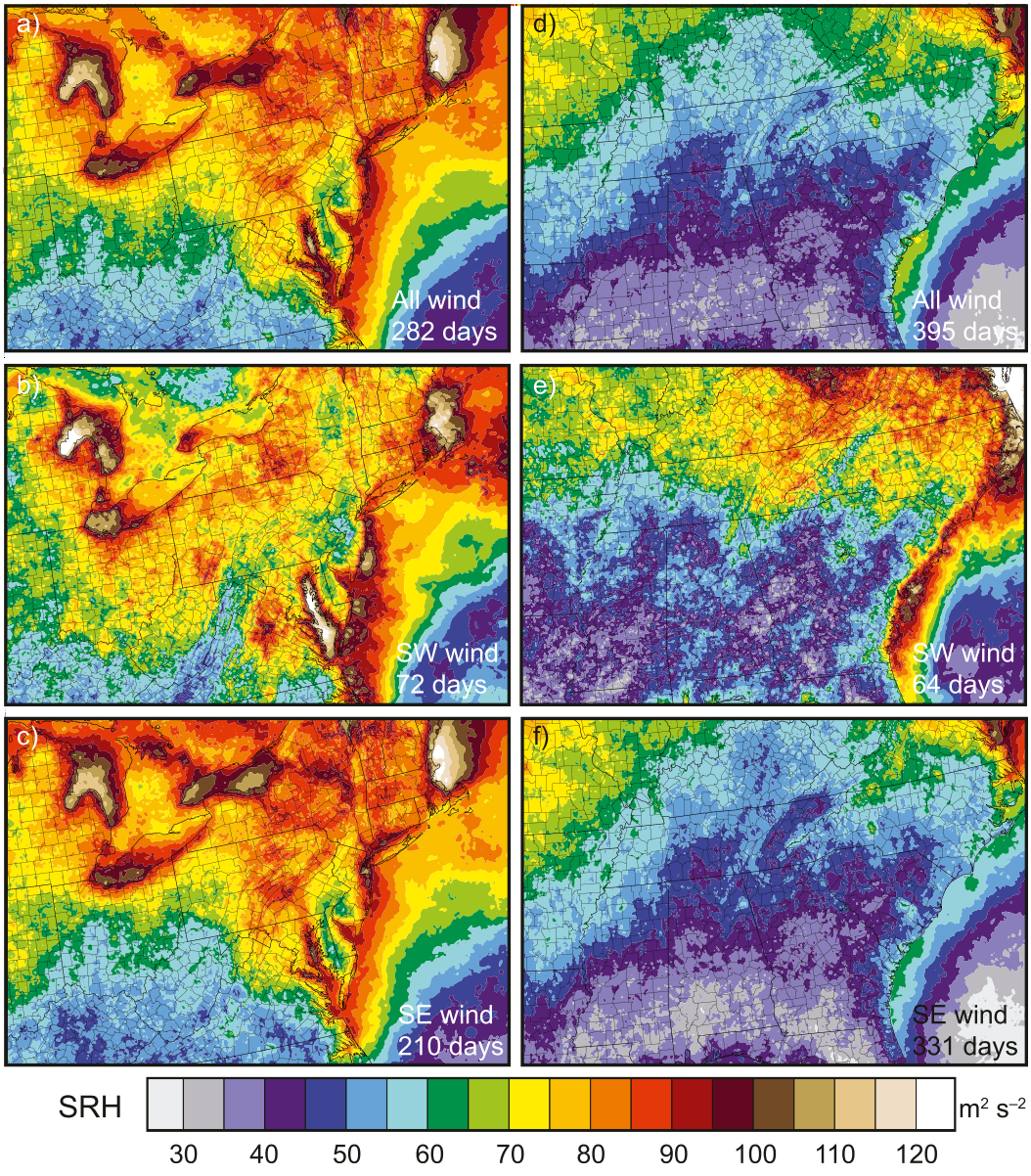

FIG. 3. As in Fig. 2, but for mean SRH01.

the wind direction affects the influence of topography. Ground-relative wind speed, vertical shear, and stratification also likely affect the influence of topography on convective storm environments. However, the sample size was not large enough to have so many subsets of data given that large sample sizes are required in order to attribute anomalies in the mean fields to topography.

3. Results

Figures 2–4 display mean fields of MLCAPE, SRH01, and STP, respectively, on convective days in the Northeast and Southeast regions.[1] All fields are shown at 2100 UTC, which is during the late afternoon hours when convective storms typically are initiated or maturing. The mean fields at other times during the afternoon through early evening (the 1800–0000 UTC time period; not shown) are qualitatively similar.

Large-scale variation in MLCAPE and SRH01 is evident in both regions, with MLCAPE generally decreasing

[1] Enlarged versions of the figures, zoomed in so that finer-scale details are more readily seen, are included in the online supplement.

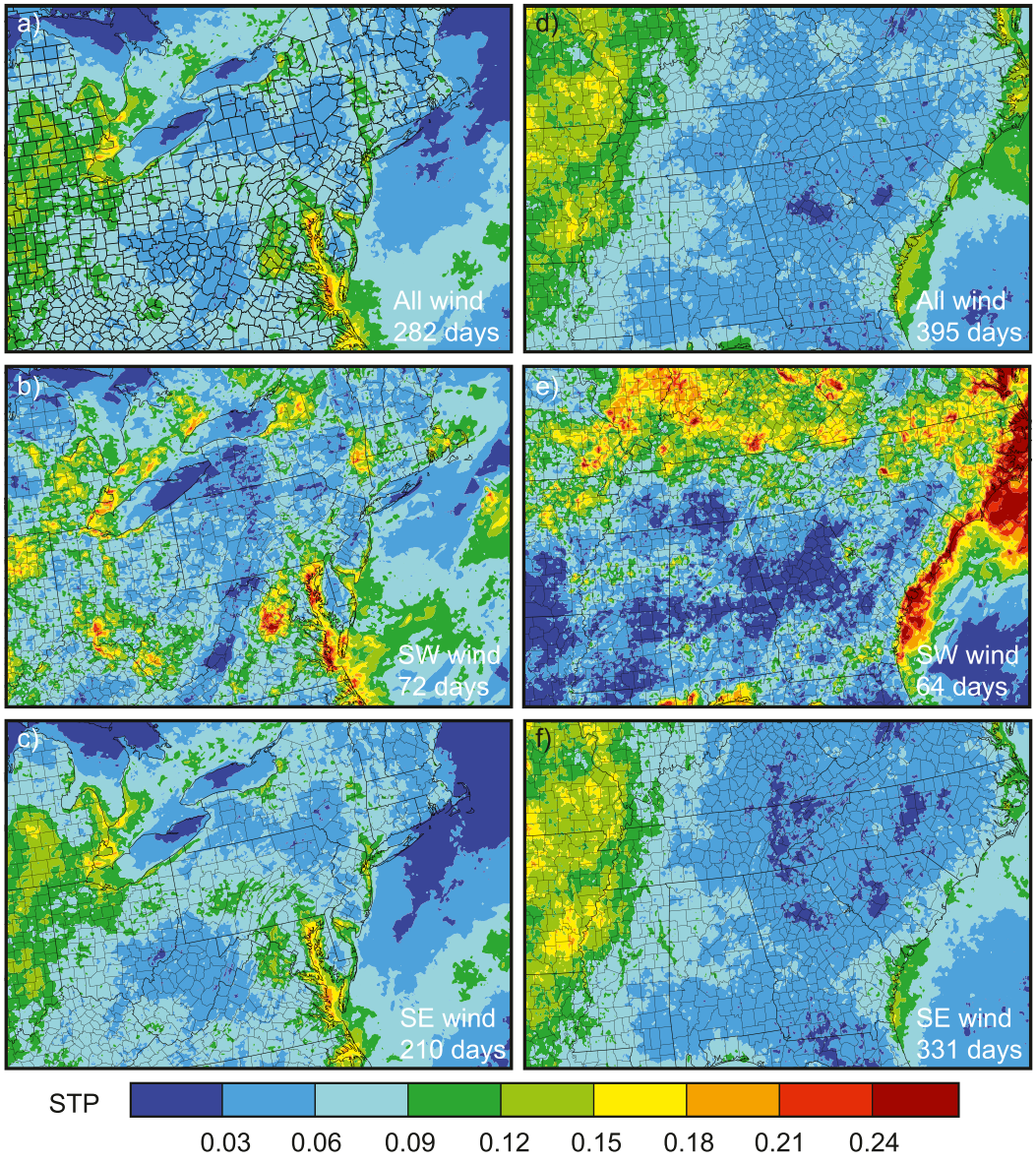

FIG. 4. As in Fig. 2, but for mean STP.

with latitude (Figs. 2a,d) and SRH01 increasing with latitude (Figs. 3a,d). The northward decrease in MLCAPE is mostly attributable to the northward decrease in boundary layer water vapor concentration (not shown), and the northward increase in SRH01 can be attributed to the northward increase in the magnitude of the tropospheric vertical wind shear, which is positively correlated with SRH01 (also not shown). No large-scale meridional variation in STP is apparent (Figs. 4a,d).

Smaller-scale anomalies are evident in the mean fields of convective parameters as well; these are the anomalies we believe are most likely attributable to topographic variability. Again, the goal of the paper is not to identify every anomaly evident in Figs. 2–4 (it would be impractical to do so). We can, however, comment on some of the most prominent anomalies.

Some of the most obvious MLCAPE anomalies are associated with cool bodies of water. For example, the MLCAPE over Lakes Erie, Ontario, and Huron is ~200 J kg^{-1} lower than over adjacent land areas at the same latitude, and the MLCAPE immediately off the East Coast (over the cool waters west of the warm Gulf Stream) is 500–800 J kg^{-1} less (Figs. 2a,d). The spatial patterns of MLCAPE anomalies are fairly similar in the SE and SW wind regimes (Figs. 2b,c,e,f).

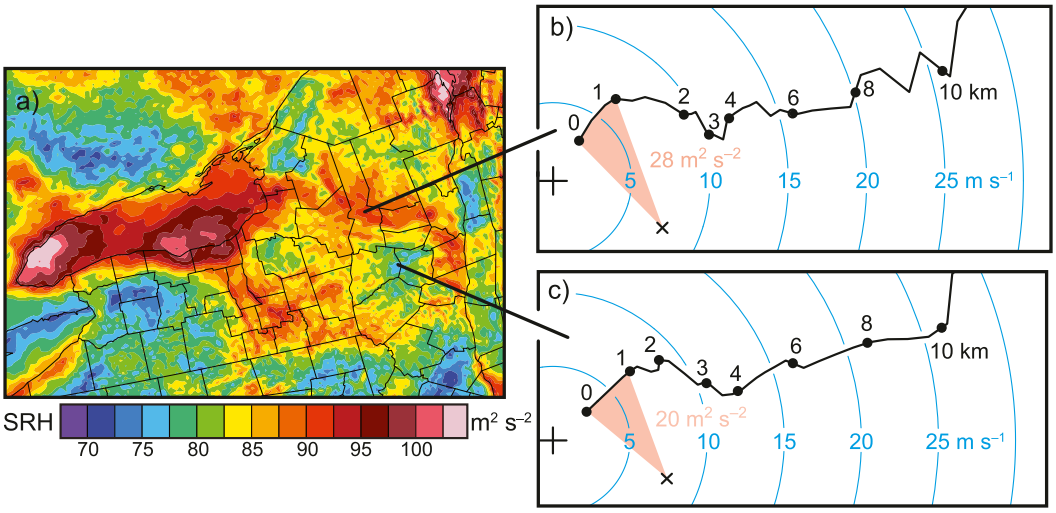

FIG. 5. (a) Mean SRH01 in New York on all convective days (the color scale differs from that used in Fig. 3a). Mean hodographs at locations within the SRH (b) maximum and (c) minimum identified in (a) [lines are drawn from the hodographs to their respective locations in (a)]. Numerals along the hodographs indicate altitudes above ground (km). The × in each panel indicates the storm motion predicted using the Bunkers et al. (2000) algorithm. The SRH01 values displayed in (b) and (c) are calculated from the mean hodographs shown in those panels. These values are significantly less than the mean SRH01 values present at the respective locations in (a). (The SRH01 obtained from the mean hodograph is not the same as the mean SRH01.)

Additional MLCAPE anomalies are present west of Washington, D.C. (MLCAPE is ~200 J kg^{-1} higher than in the immediate surroundings; Figs. 2a–c); southeast of Atlanta, Georgia (MLCAPE is 200–400 J kg^{-1} higher than in the immediate surroundings, particularly in SW low-level flow; Fig. 2e); and along the spine of the Appalachian Mountains (MLCAPE is 200–400 J kg^{-1} lower than at adjacent lower altitudes; Figs. 2a,d).

SRH01 anomalies are found on the coasts of large bodies of water. The southern coasts of the Great Lakes (Fig. 3a), the western shore of the Chesapeake Bay (Fig. 3a), and the southern Atlantic Coast (especially under SW low-level flow; Fig. 3e) all experience SRH01 values that are ~30 m^2 s^{-2} higher than areas farther onshore. The increase in SRH01 along the shores of bodies of water is due to the baroclinic generation of horizontal vorticity along these shores that has a component aligned with the low-level inflow of a potential storm.

Spatial patterns of SRH01 anomalies differ in the SE and SW flow regimes. SRH01 in parts of New York's Mohawk Valley is 10–15 m^2 s^{-2} lower than at adjacent higher altitudes in SW low-level flow (Fig. 3b) and becomes 10–15 m^2 s^{-2} greater than adjacent higher altitudes in SE low-level flow (Fig. 3c). The location of SRH01 anomalies along the coasts of the Great Lakes also depends on the low-level flow direction (Figs. 3b,c).

As an example of what further analysis can be undertaken to explore the origins of a localized anomaly, mean wind hodographs inside and just outside of the SRH01 enhancement within the Mohawk Valley are presented in Fig. 5. While the predicted storm motion is similar in both hodographs, a decrease in surface wind speed and an increase in 0–1-km winds within the anomaly (Fig. 5b) lengthens the hodograph and increases SRH01, whereas this 0–1-km wind speed enhancement is absent in the immediate surroundings (Fig. 5c). The SRH01 values displayed in each hodograph (Figs. 5b,c) are derived from the mean wind values and not those from the mean SRH01 field (Fig. 5a); the difference between SRH01 calculated from the hodograph versus the mean field is large. Such a large difference is expected, as averaging over many different wind regimes yields a mean wind hodograph without much SRH01. The differences between the mean hodographs are extremely subtle. It is important to recognize that a topographically generated anomaly that might be observed *on a specific day* is virtually guaranteed to be larger in amplitude than the anomalies present in the mean fields, given that an anomaly's position relative to a topographic feature would likely shift slightly from day to day, depending on the mean wind speed and direction (and perhaps other factors as well). The averaging undertaken herein smears the daily anomalies such that the anomalies in the mean fields necessarily are broader and weaker than topographically generated anomalies on a specific day.

With respect to the mean fields of STP, the horizontal heterogeneity is larger on the SW-flow days than

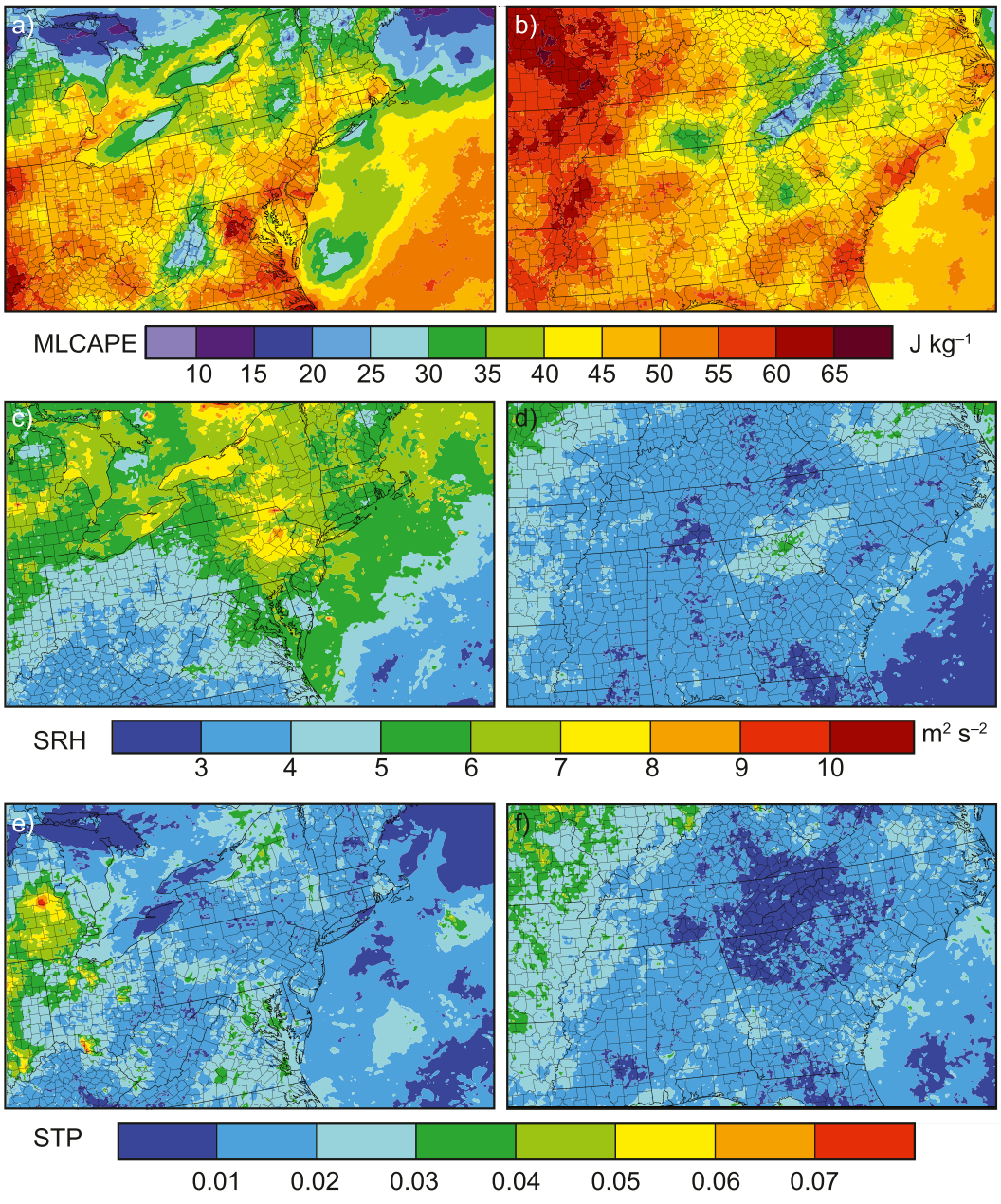

FIG. 6. Bootstrapped standard errors for each of the convective parameters in the (a),(c),(e) Northeast and (b),(d),(f) Southeast regions for all convective days.

SE-flow days (though the sample size is smaller for SW-flow days), especially in the southeastern domain (Figs. 4e,f; note especially the heterogeneity in SW flow from Mississippi to Georgia). Among the most obvious regions where STP is enhanced are those along and offshore of the southeastern U.S. coastline in SW low-level flow (Fig. 4e), and in the western portion of the southeastern U.S. domain, particularly in SE low-level flow (Figs. 4d,f). More subtle local enhancements of STP are present in the flat terrain east of Lake Ontario and within the Hudson and Mohawk Valleys, especially on SW-flow days (Figs. 4a,b). This part of Ontario, Canada, is known to be a local ''hotspot'' for tornadoes (Etkin et al. 2001), and the Hudson and Mohawk Valleys have been speculated in some prior studies as being a region favorable for tornadoes owing to a terrain influence (LaPenta et al. 2005; Bosart et al. 2006; Tang et al. 2016). Many other pockets of enhanced STP are evident in Fig. 4; again, it is impractical to identify every anomaly, nor can we say whether any of the

anomalies would have a noticeable influence on a convective storm.

To assess the statistical significance of the anomalies in the mean fields, standard errors are estimated using bootstrap resampling (Efron 1982; Efron and Tibshirani 1993). Each region contains a set of n convective days. From this set of convective days, n samples are randomly drawn with replacement, and the mean of each convective parameter for this given set is then calculated. This process is repeated 10 000 times, and the standard deviation of these 10 000 new means can be interpreted as the bootstrapped standard error (Fig. 6). A particular anomaly in a mean field can be regarded as being statistically significant if it differs from neighboring values (i.e., the values that one could reasonably assume would be present if the anomaly were removed) by more than the bootstrapped standard error at the location of the anomaly in question. The vast majority of the meso-β-scale anomalies evident in Figs. 2–4 are statistically significant.[2]

4. Summary, conclusions, and future work

In this paper, parameters used in severe storm forecasting to assess instability, vertical wind shear, and the likelihood of tornadoes were obtained from the HRRR and averaged over a period of three warm seasons to investigate whether there are regularly occurring anomalies in the parameters. Though there is, not surprisingly, a large-scale meridional gradient in the parameters (e.g., instability decreases and vertical shear increases to the north) owing to the large-scale meridional temperature and pressure gradient, smaller-scale anomalies also were identified in many locations in the eastern United States. These anomalies are likely attributable to the influence of topography; many of the anomalies were aligned with lakeshores, coastlines, valleys, and ridges. Many local minima and maxima in the convective environment parameters can be regarded as being statistically significant in the sense that their amplitudes exceed bootstrapped estimates of the standard errors of the parameters obtained in the same regions.

We envision that the climatologies presented here will be useful for directing targeted observations in future field campaigns, such as VORTEX-SE, as well as guiding numerical simulations (using more realistic terrain and storms than in past idealized simulations) designed to investigate if and how storms are affected by topographically generated environmental heterogeneity. Such simulations will likely need finer resolution than the HRRR. Though the HRRR is capable of resolving at least the largest-scale influences of topography on the convective storm *environment*, 3-km horizontal grid spacing is probably too coarse to faithfully simulate possible responses of a *storm* to a changing environment. Future work also should include 1) efforts to better understand the dynamical and thermodynamical origins of the anomalies in instability, shear, etc.; 2) higher-order statistical processing techniques such as principal component analysis to determine spatial modes of variability; and 3) perhaps also the exploration of different ways of binning the data. For example, convective parameters could be averaged over bins defined by wind speed, wind shear, or static stability, or perhaps narrower ranges of wind directions could be used than have been used herein. The challenge is in obtaining a sufficiently large sample so that day-to-day variability vanishes, though using more than about three years' worth of model data might also prove challenging because this is roughly the time scale on which major changes are made to models.

Acknowledgments. This work was supported by NOAA Collaborative Science, Technology, and Applied Research (CSTAR) Program Award NA14NWS4680015 made to The Pennsylvania State University. We thank Drs. Yvette Richardson and Matthew Kumjian for their suggestions during the course of this work, and we also are grateful for the comments made by Dr. Matthew Bunkers and one anonymous reviewer. This work would not have been possible without the generous computer support provided by Art Person.

[2] Additional standard error fields are included in the online supplement.

REFERENCES

Benjamin, S., and Coauthors, 2016: A North American hourly assimilation and model forecast cycle: The Rapid Refresh. *Mon. Wea. Rev.*, **144**, 1669–1694, doi:10.1175/MWR-D-15-0242.1.

Bosart, L. F., A. Seimon, K. D. LaPenta, and M. J. Dickinson, 2006: Supercell tornadogenesis over complex terrain: The Great Barrington, Massachusetts, tornado on 29 May 1995. *Wea. Forecasting*, **21**, 897–922, doi:10.1175/WAF957.1.

Bunkers, M. J., B. A. Klimowski, J. W. Zeitler, R. L. Thompson, and M. L. Weisman, 2000: Predicting supercell motion using a new hodograph technique. *Wea. Forecasting*, **15**, 61–79, doi:10.1175/1520-0434(2000)015<0061:PSMUAN>2.0.CO;2.

Ćurić, M., D. Janc, and V. Vučković, 2007: Numerical simulation of Cb cloud vorticity. *Atmos. Res.*, **83**, 427–434, doi:10.1016/j.atmosres.2005.10.024.

Davies-Jones, R. P., D. W. Burgess, and M. Foster, 1990: Test of helicity as a forecast parameter. Preprints, *16th Conf. on Severe Local Storms*, Kananaskis Park, AB, Canada, Amer. Meteo. Soc., 588–592.

Efron, B., 1982: *The Jackknife, the Bootstrap, and Other Resampling Plans*. CBMS-NSF Regional Conference Series in Applied Math, Vol. 38, Society for Industrial and Applied Mathematics, 92 pp.

——, and R. J. Tibshirani, 1993: *An Introduction to the Bootstrap*. Chapman and Hall, 436 pp.

Etkin, D., S. E. Brun, A. Shabbar, and P. Joe, 2001: Tornado climatology of Canada revisited: Tornado activity during different phases of ENSO. *Int. J. Climatol.*, **21**, 915–938, doi:10.1002/joc.654.

Frame, J., and P. Markowski, 2006: The interaction of simulated squall lines with idealized mountain ridges. *Mon. Wea. Rev.*, **134**, 1919–1941, doi:10.1175/MWR3157.1.

Homar, V., M. Gayà, R. Romero, C. Ramis, and S. Alonso, 2003: Tornadoes over complex terrain: An analysis of the 28th August 1999 tornadic event in eastern Spain. *Atmos. Res.*, **67–68**, 301–317, doi:10.1016/S0169-8095(03)00064-4.

LaPenta, K. D., L. F. Bosart, T. J. Galarneau Jr., and M. J. Dickinson, 2005: A multiscale examination of the 31 May 1998 Mechanicville, New York, tornado. *Wea. Forecasting*, **20**, 494–516, doi:10.1175/WAF875.1.

Markowski, P. M., and Y. Richardson, 2006: On the classification of vertical wind shear as directional shear versus speed shear. *Wea. Forecasting*, **21**, 242–247, doi:10.1175/WAF897.1.

——, and N. Dotzek, 2011: A numerical study of the effects of orography on supercells. *Atmos. Res.*, **100**, 457–478, doi:10.1016/j.atmosres.2010.12.027.

Reeves, H. D., and Y.-L. Lin, 2007: The effects of a mountain on the propagation of a preexisting convective system for blocked and unblocked flow regimes. *J. Atmos. Sci.*, **64**, 2401–2421, doi:10.1175/JAS3959.1.

Smith, T. L., S. G. Benjamin, J. M. Brown, S. Weygandt, T. Smirnova, and B. Schwartz, 2008: Convection forecasts from the hourly updated, 3-km High Resolution Rapid Refresh (HRRR) model. Preprints, *24th Conf. on Severe Local Storms*, Savannah, GA, Amer. Meteor. Soc., 11.1. [Available online at https://ams.confex.com/ams/pdfpapers/142055.pdf.]

Soderholm, B., B. Ronalds, and D. J. Kirshbaum, 2014: The evolution of convective storms initiated by an isolated mountain ridge. *Mon. Wea. Rev.*, **142**, 1430–1451, doi:10.1175/MWR-D-13-00280.1.

Tang, B., M. Vaughn, R. L. Azear, K. Corbosiero, L. Bosart, T. Wasula, I. Lee, and K. Tipton, 2016: Topographic and boundary influences on the 22 May 2014 Duanesburg, New York, tornadic supercell. *Wea. Forecasting*, **31**, 107–127, doi:10.1175/WAF-D-15-0101.1.

Teng, J.-H., C.-S. Chen, T.-C. C. Wang, and Y.-L. Chen, 2000: Orographic effects on a squall line system over Taiwan. *Mon. Wea. Rev.*, **128**, 1123–1138, doi:10.1175/1520-0493(2000)128<1123:OEOASL>2.0.CO;2.

Thompson, R. L., R. Edwards, J. A. Hart, K. L. Elmore, and P. M. Markowski, 2003: Close proximity soundings within supercell environments obtained from the Rapid Update Cycle. *Wea. Forecasting*, **18**, 1243–1261, doi:10.1175/1520-0434(2003)018<1243:CPSWSE>2.0.CO;2.